Antibody Therapeutics, 2022, Vol. 5, No. 3 ***226–231***
https://doi.org/10.1093/abt/tbac020
Advance Access Publication on 8 February 2022

Brief Report

Pan-cancer distribution of cleaved cell-surface amphiregulin, the target of the GMF-1A3 antibody drug conjugate

Kristopher A. Lofgren[1], Nicolette C. Reker[1], Sreeja Sreekumar[1] and Paraic A. Kenny[1,2,*]

[1]Kabara Cancer Research Institute, Gundersen Medical Foundation, La Crosse, WI 54601, USA , and [2]Department of Medicine, University of Wisconsin School of Medicine and Public Health, Madison, WI 53705, USA

Received: March 24, 2022; Revised: July 8, 2022; Accepted: July 28, 2022

ABSTRACT

Amphiregulin is a transmembrane protein which, when cleaved by the TACE/ADAM17 protease, releases a soluble epidermal growth factor receptor ligand domain that promotes proliferation of normal and malignant cells. We previously described a rabbit monoclonal antibody, GMF-1A3, that selectively recognizes the cell-associated cleaved amphiregulin epitope. Antibody-drug conjugates had anti-tumor activity against human breast cancer xenografts. Several tumor types express amphiregulin, but evidence for a functional requirement for amphiregulin in these malignancies is limited. By directly evaluating amphiregulin cleavage with immunohistochemistry, GMF-1A3 provides a more direct measure of amphiregulin activity. Using 370 specimens from 10 tumor types (as well as normal controls), we demonstrate that cleaved amphiregulin is widely expressed in solid tumors and is especially common (> 50% of cases) in breast, prostate, liver and lung cancer. As a potential companion diagnostic for this antibody-drug conjugate, this assay allows identification of tumors with high levels of the cleaved amphiregulin target.

Statement of Significance: We demonstrate that amphiregulin cleavage is a prevalent event in breast, prostate, liver and lung cancer, significantly expanding the repertoire of tumor types in which antibody-drug conjugates based on GMF-1A3 might be evaluated for clinical efficacy.

KEYWORDS: tissue microarray; amphiregulin; monomethyl auristatin E; antibody-drug conjugate

INTRODUCTION

Amphiregulin (AREG) is a transmembrane protein which, following TACE/ADAM17-dependent cleavage [1], releases a soluble epidermal growth factor receptor (EGFR) ligand domain which promotes proliferation of normal and malignant cells. This proteolysis event leaves a residual cell-surface transmembrane stalk which is subsequently internalized. We determined the N-terminal sequence of this cell-associated AREG cleavage product [2] and generated antibodies that selectively recognize this epitope in its cleaved but not its intact conformation, as demonstrated in experiments with synthetic peptides and against AREG endogenously expressed and cleaved in live cells [3]. The antibodies are internalized by cultured cells in a cleaved AREG-dependent manner [3]. We have developed one of these antibodies into a monomethyl auristatin E (MMAE)-based antibody-drug conjugate, GMF-1A3, and demonstrated that it can kill human breast cancer cells in vitro and as xenografts in immunocompromised mice when it binds to, and is internalized with, the cell surface AREG stalk during its physiological degradation process [3].

Appropriate selection of patients for targeted cancer treatment typically relies on some kind of companion diagnostic to identify the sub-population of patients whose tumors are most likely to respond. An initial evaluation of our GMF-1A3 antibody as a potential

*To whom correspondence should be addressed. Paraic A. Kenny. Email: pakenny@gundersenhealth.org

immunohistochemical companion diagnostic was performed in 138 breast cancer specimens. We found medium/high immunoreactivity in 70% of cases [3]. Although our initial drug development focus has been on AREG in breast cancer, AREG is expressed in several other cancer types [4] so the potential utility of therapeutic antibody drug conjugates likely extends to other malignancies. Although the expression of AREG in these other tissues has been described, the extent to which cleaved AREG is present at sufficient abundance to potentially represent a viable target for the GMF-1A3-MMAE antibody drug conjugate is unknown. To address this issue, we have evaluated the levels of cleaved AREG in tissue microarrays comprised of 370 specimens from a total of 10 tumor types. In parallel, we examined the abundance of cleaved AREG in 93 specimens from a total of 20 normal tissues.

MATERIALS AND METHODS

Immunohistochemistry

Two multiple organ carcinoma tissue microarrays (TMA) were purchased from BioCoreUSA (Philadelphia, PA, USA). A tissue microarray of non-malignant tissues was obtained from US Biomax (Derwood, MD, USA). The slides were deparaffinized in xylene and rehydrated by serial incubations in graded ethanol and then in water in a Histo-Tek® SL Slide Stainer (Sakura Finetek USA, Inc., Torrance, CA, USA). Antigen retrieval was performed in a steamer by boiling the slides in a container of citrate buffer (pH 6.0) for 20 min which was then removed for 15 min of cooling on the benchtop. The slides were washed in 1× Wash buffer (Dako Agilent, Santa Clara, CA, USA) and endogenous peroxidase was quenched by incubating with Dako Dual Endogenous Enzyme Block for 10 min. The slides were again washed in 1× Wash buffer, blocked (5% rabbit/10% goat serum in PBS) and immunostained with goat anti-AREG antibody (15 μg/mL; AF262, R&D Systems) or rabbit anti-cleaved AREG 1A3 antibody (10 μg/mL) overnight at 4°C. The slides were washed four times in 1× Wash buffer, followed by incubation for 45 min at room temperature in 1:100 dilution of rabbit anti-goat immunoglobulins/horseradish peroxidase (HRP) or ready-to-use goat anti-rabbit HRP-labelled polymer (Dako). The slides were washed twice in 1× Wash buffer and the color was developed with 3,3-diaminobenzidine tetrahydrochloride substrate chromogen system (DAKO). Sections were washed with water and counterstained with hematoxylin, rinsed with water, dehydrated by serial ethanol washes to 100%, cleared and mounted in Permount (Thermo Fisher Scientific). The staining intensity was assessed semi-quantitatively using a four-point scale (Negative = 0, Low = 1, Medium = 2, High = 3) by two investigators working independently on blinded samples. Discordant scores were resolved by joint review. The tumor tissue array design included 380 cores. In the TMA sections used, 370 cores were evaluable for cleaved AREG (Fig. 1A and B) and 369 were evaluable for both cleaved and total AREG (Fig. 1C and D). The normal tissue array included 100 cores from 20 tissues, of which 93 cores were evaluable for cleaved AREG.

RESULTS

Tissue distribution of cleaved AREG in cancer

To broadly evaluate the levels of cleaved AREG in cancer, we performed immunohistochemistry on multi-tumor tissue microarrays. The neoplastic compartment of each specimen was scored semi-quantitatively as negative (0), low [1], medium [2] or high [3]. No neoplastic cells were negative for 1A3 immunostaining. Representative examples of each staining score are shown in Figure 1A, and data from all tissues examined are summarized in Figure 1B. A circumferential staining pattern was especially evident in the high-intensity specimens (Fig. 1A, right). At least 50% of breast, prostate, liver and lung tumors were stained with the highest score for cleaved AREG.

Cross-comparison of levels of total and cleaved AREG in cancer

The specificity of the GMF-1A3 antibody for cleaved AREG was previously verified by the evaluation of cross-reactivity against peptides representing cleaved and full-length AREG [3]. If GMF-1A3 antibody immunohistochemistry also accurately reflects cleaved AREG levels in formalin-fixed tissue then we would anticipate that intensity scores for both GMF-1A3 and total AREG would tend to have a positive relationship and, in particular, that cases with low-to-absent expression of total AREG should be very unlikely to exhibit robust immunostaining with GMF-1A3. Furthermore, because of our intention to evaluate potential utility of GMF-1A3 as an antibody-drug conjugate, we evaluated whether there might be a substantial fraction of AREG high tumors that have negligible levels of cleaved AREG (potentially due to either low rates of cleavage or rapid rates of internalization/degradation) which might indicate insufficient cell surface cleaved AREG for efficient targeting. We immunostained the tumor tissue microarray with an antibody against total AREG and cross-compared the intensity scores for each antibody. Data from all tissues are summarized in Figure 1C and D, and data from individual tissues are shown in Figure 2.

As anticipated, there was a generally positive relationship between total AREG levels and levels of cleaved AREG (Figs 1C and 2). All specimens had at least some AREG immunoreactivity and only 16/369 specimens had the highest score for cleaved AREG and the lowest score (but not negative) for total AREG. Only 1/369 specimens had the highest score for total AREG and the lowest score for cleaved AREG. We also noted that cleaved AREG and total AREG immunoreactivity were found together in the same tissue compartment (e.g., representative example of medium intensity immunostaining in Fig. 1D). Together, these suggest that the GMF-1A3 antibody detects cleaved AREG in formalin-fixed paraffin-embedded tissue with minimal non-specific immunostaining, and that levels of cleaved AREG likely necessary to act as an in vivo target for an antibody drug conjugate are commonly found in tumors with medium-to-high levels of total AREG. Although we observed a departure from a linear positive relationship between the pair-wise scores (most prominently in breast,

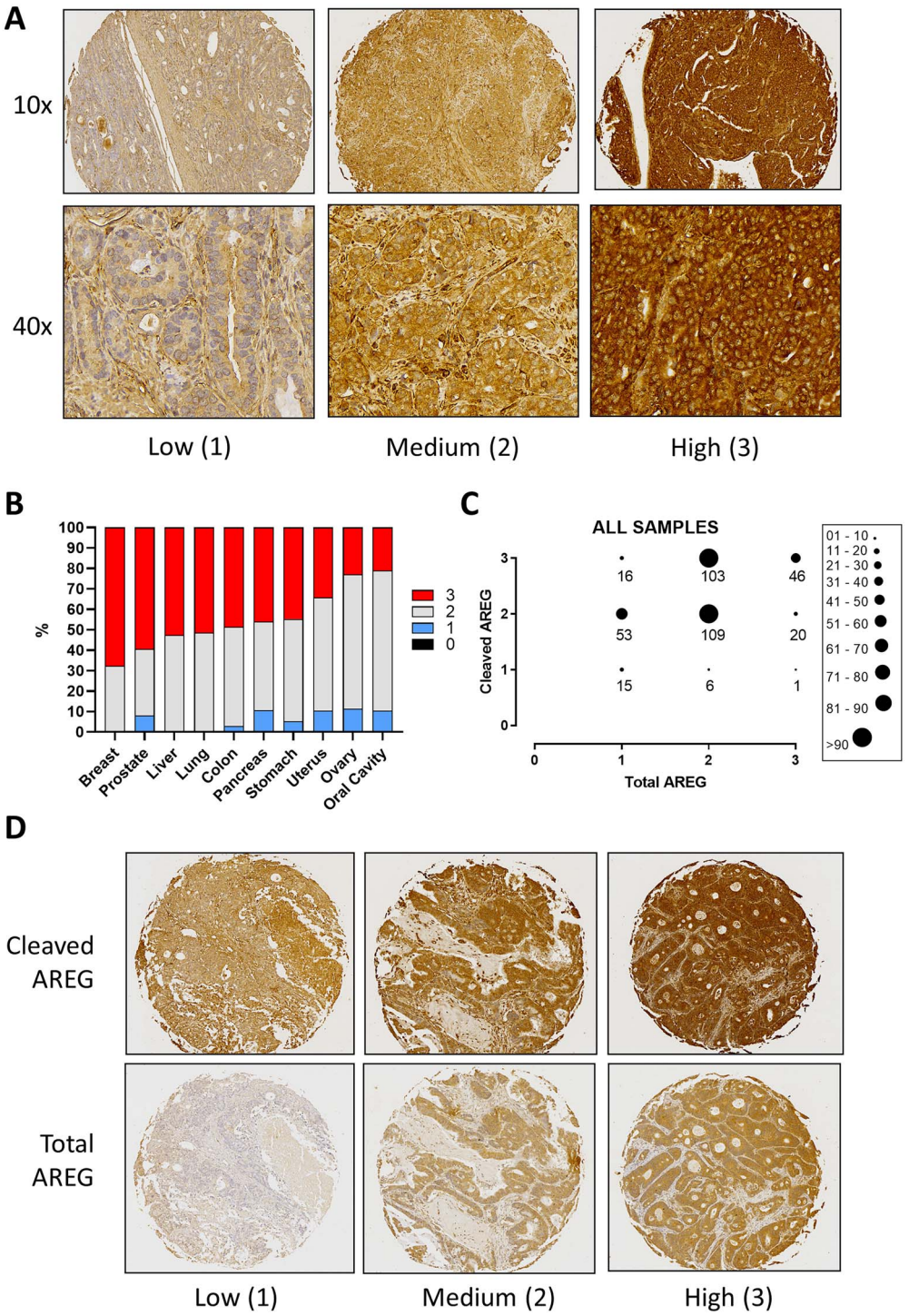

Figure 1. Tissue distribution of cleaved AREG in solid tumors. (A). Representative examples of immunohistochemical staining for cleaved AREG at each of the three detected staining intensities. Images from the same cores were captured at 10× and 40× magnification. (B). Quantification of cleaved AREG intensity scores in 380 tumors from 10 different cancer types. (C). Cross-comparison of intensity scores for both cleaved (Y-axis) and total (X-axis) AREG in 369 tumors. Data point size is proportional to the number of cases in each pairwise group and the number of cases in each group is indicated. (D). Representative examples of tissue cores in which both total and cleaved AREG both had low, medium or high immunostaining intensity.

prostate, liver and lung, Fig. 2), it was in specimens having the highest intensity score for cleaved AREG with a medium score for total AREG, suggesting particularly active levels of AREG processing in these tumors.

We then assessed the distribution of cleaved AREG in tissue microarrays of cancer-free tissues using an identical scoring strategy (Fig. 3). Cleaved AREG was detected in all tissue types examined. Of 93 cores evaluated, only

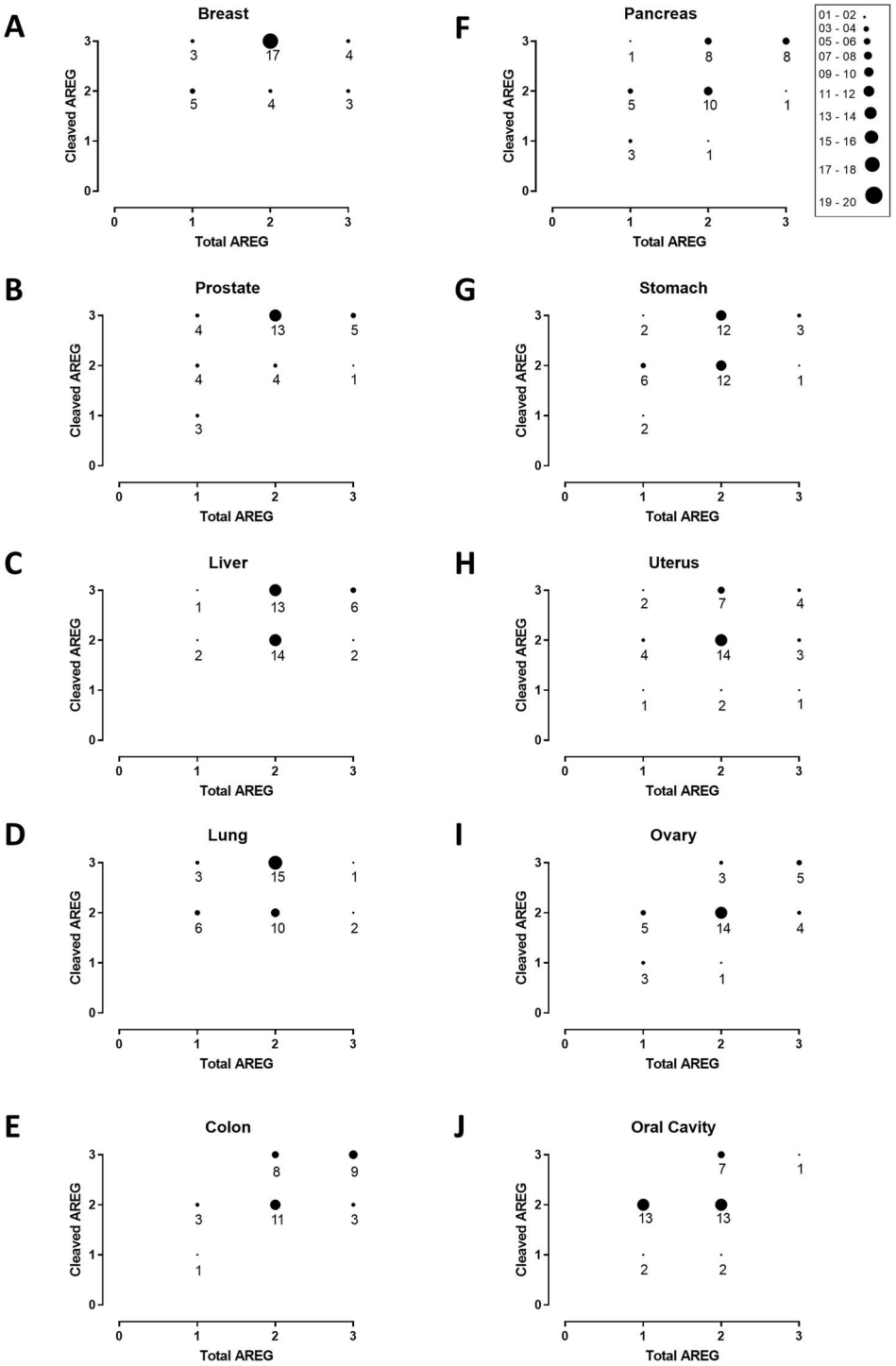

Figure 2. Pairwise comparison of cleaved and total AREG levels in 10 tumor types. (A–J) Cross-comparison of intensity scores for both cleaved (Y-axes) and total (X-axes) AREG in each of the 10 indicated tumor types. Data point size is proportional to the number of cases in each pairwise group and the number of cases in each group is indicated.

seven specimens (7.5%) were scored in the highest intensity group; 60.2% of specimens (56 cases) were scored at the intermediate intensity level. Among the epithelial organs examined, cleaved AREG detection was typically restricted to the epithelial compartment, whereas it was detected in lymphoid and hematopoietic cells in the spleen, bone marrow and lymph node. It was diffusely detected in the cerebrum.

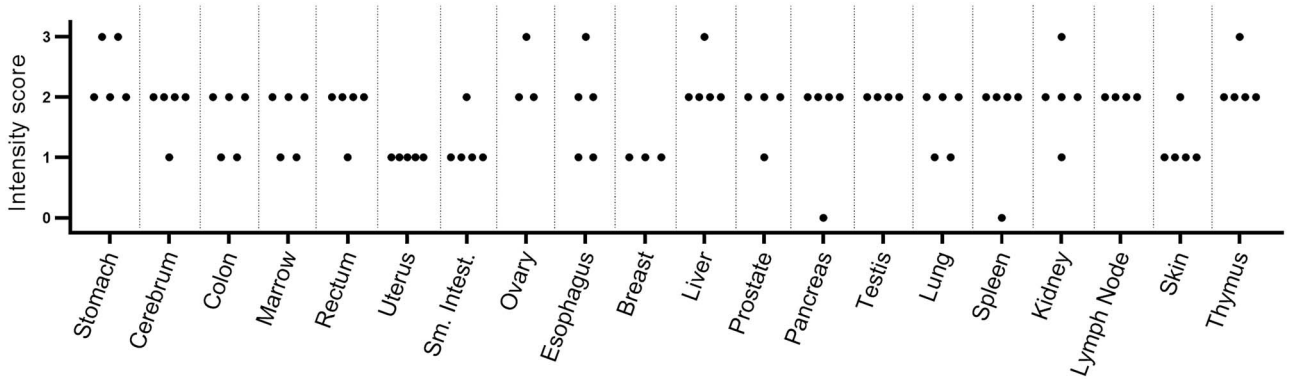

Figure 3. Cleaved AREG levels in 20 normal human tissues. Cleaved AREG immunostaining was quantified using an identical scoring scheme to the tumor tissue microarrays.

DISCUSSION

In this study, we extended our prior findings in breast cancer specimens [3] to several additional malignancies, showing that AREG expression is widespread and, when expressed at moderate to high levels, AREG cleavage was commonly detected in these specimens. This substantially extends the tumor repertoire where the cleaved AREG target of the GMF-1A3-MMAE antibody drug conjugate is commonly expressed.

Expression of total AREG in several of these tumors had previously been described [5–9], but evidence for a functional requirement for AREG has been limited to a smaller group, including colorectal [10] and breast cancer [6, 11]. In parallel, our studies in normal tissues highlight the prevalence of AREG cleavage during normal tissue homeostasis. These data may be useful in considering whether an appropriate therapeutic index with an antibody drug conjugate can be achieved and what modifications to either chemotherapeutic cargo or linker might be helpful.

Our demonstration here that the expressed AREG is being actively cleaved in a wide range of cancer types confirms that autocrine AREG signaling following ADAM17-dependent AREG cleavage is commonly occurring, raising the possibility that AREG-dependent EGFR activation may be a more frequent mitogenic signal that has been previously appreciated. Accordingly, in addition to being potentially useful as a companion diagnostic to select patients for treatment with GMF-1A3-MMAE, this antibody may facilitate a more complete appraisal of the extent of active autocrine AREG/EGFR signaling in both normal tissue development and homeostasis as well as cancer initiation and progression.

In general, "on-target/off-tumor" toxicities are a common feature of antibody drug conjugates targeting solid tumors due to the targets being tumor-associated as opposed to tumor-restricted. For example, off-tumor ERBB2 expression is found in normal breast, thyroid, endometrium, kidney and colon [12], yet clinical efficacy is seen with both trastuzumab emtansine [13] and trastuzumab deruxtecan [14]. Notably, trastuzumab deruxtecan has efficacy even in ERBB2-low tumors [15] which, presumably, have expression levels quite similar to those found in normal tissues. Similarly, TROP2 is expressed in skin, uterus, bladder, oral mucosa, nasopharynx and lungs [16], yet sacituzumab govitecan, an SN38 conjugate, is approved for triple-negative breast cancer [17]. Finally, LIV1 is widely expressed in normal tissues [18] but the MMAE conjugate targeting it, ladiratuzumab vedotin, was tolerable and had clinical efficacy in triple-negative breast cancer patients [19]. These prior experiences emphasize the importance of being aware of the potential for off-target toxicities but suggest that the ability to vary payloads, linkers and dosing may allow the identification of tolerable and clinically effective targeting strategies for many antibodies for which the targets are not tumor-restricted [16].

FUNDING

This study was supported by the Department of Defense Breast Cancer Research Program (W81XWH-14-1-0294 to P.K.), the American Cancer Society (123001-RSG-12-267-01-TBE to P.K.) and the Gundersen Medical Foundation. K.L. was supported by the Norman L. Gillette, Jr. Breast Cancer Research Fellowship. PK holds the Dr. Jon and Betty Kabara Endowed Chair of Precision Oncology.

CONFLICT OF INTEREST

K.L., S.S. and P.K. are inventors on a patent application (US 17/836,517) describing the antibodies used in this manuscript.

DATA AVAILABILITY

Whole slide images of the immunostained tissue microarrays are available upon request.

AUTHOR CONTRIBUTIONS

Conceptualization (P.K.), Methodology (S.S., K.L., N.R.), Investigation (K.L., N.R.), Data Analysis (K.L., N.R., P.K.), Writing—original draft preparation (K.L., P.K.),

Writing—review and editing (P.K., K.L., N.R., S.S.), Funding Acquisition (P.K.).

ETHICS & CONSENT

Consent was not required for this study.

ANIMAL RESEARCH STATEMENT

Not Applicable.

REFERENCES

1. Gschwind, A, Hart, S, Fischer, OM *et al.* TACE cleavage of proamphiregulin regulates GPCR-induced proliferation and motility of cancer cells. *EMBO J* 2003; **22**: 2411–21.
2. Levano, KS, Kenny, PA. Clarification of the C-terminal proteolytic processing site of human Amphiregulin. *FEBS Lett* 2012; **586**: 3500–2.
3. Lofgren, KA, Sreekumar, S, Jenkins, EC Jr *et al.* Anti-tumor efficacy of an MMAE-conjugated antibody targeting cell surface TACE/ADAM17-cleaved Amphiregulin in breast cancer. *Antib Ther* 2021; **4**: 252–61.
4. Busser, B, Sancey, L, Brambilla, E *et al.* The multiple roles of amphiregulin in human cancer. *Biochim Biophys Acta* 2011; **1816**: 119–31.
5. Bostwick, DG, Qian, J, Maihle, NJ. Amphiregulin expression in prostatic intraepithelial neoplasia and adenocarcinoma: a study of 93 cases. *Prostate* 2004; **58**: 164–8.
6. Peterson, EA, Jenkins, EC, Lofgren, KA *et al.* Amphiregulin is a critical downstream effector of estrogen signaling in ER alpha-positive breast cancer. *Cancer Res* 2015; **75**: 4830–8.
7. Wang, B, Yong, H, Zhu, H *et al.* Abnormal amphiregulin expression correlates with gastric cancer prognosis. *Oncotarget* 2016; **7**: 76684–92.
8. Wang, L, Wu, H, Wang, L *et al.* Expression of amphiregulin predicts poor outcome in patients with pancreatic ductal adenocarcinoma. *Diagn Pathol* 2016; **11**: 60.
9. Yonesaka, K, Zejnullahu, K, Lindeman, N *et al.* Autocrine production of amphiregulin predicts sensitivity to both gefitinib and cetuximab in EGFR wild-type cancers. *Clin Cancer Res* 2008; **14**: 6963–73.
10. Khambata-Ford, S, Garrett, CR, Meropol, NJ *et al.* Expression of epiregulin and amphiregulin and K-ras mutation status predict disease control in metastatic colorectal cancer patients treated with cetuximab. *J Clin Oncol* 2007; **25**: 3230–7.
11. Meier, DR, Girtman, MA, Lofgren, KA *et al.* Amphiregulin deletion strongly attenuates the development of estrogen receptor-positive tumors in p53 mutant mice. *Breast Cancer Res Treat* 2020; **179**: 653–60.
12. Natali, PG, Nicotra, MR, Bigotti, A *et al.* Expression of the p185 encoded by HER2 oncogene in normal and transformed human tissues. *Int J Cancer* 1990; **45**: 457–61.
13. Verma, S, Miles, D, Gianni, L *et al.* Trastuzumab emtansine for HER2-positive advanced breast cancer. *N Engl J Med* 2012; **367**: 1783–91.
14. Modi, S, Saura, C, Yamashita, T *et al.* Trastuzumab deruxtecan in previously treated HER2-positive breast cancer. *N Engl J Med* 2020; **382**: 610–21.
15. Modi, S, Jacot, W, Yamashita, T *et al.* Trastuzumab deruxtecan in previously treated HER2-low advanced breast cancer. *N Engl J Med* 2022; **387**: 9–20.
16. Criscitiello, C, Morganti, S, Curigliano, G. Antibody-drug conjugates in solid tumors: a look into novel targets. *J Hematol Oncol* 2021; **14**: 20.
17. Bardia, A, Mayer, IA, Vahdat, LT *et al.* Sacituzumab govitecan-hziy in refractory metastatic triple-negative breast cancer. *N Engl J Med* 2019; **380**: 741–51.
18. Taylor, KM, Morgan, HE, Johnson, A *et al.* Structure-function analysis of LIV-1, the breast cancer-associated protein that belongs to a new subfamily of zinc transporters. *Biochem J* 2003; **375**: 51–9.
19. Han, H, Diab, S, Alemany, C *et al.* Abstract PD1-06: Open label phase 1b/2 study of ladiratuzumab vedotin in combination with pembrolizumab for first-line treatment of patients with unresectable locally-advanced or metastatic triple-negative breast cancer. *Cancer Res* 2020; **80**: PD1-06.